

## DYNAMIC DEFORMATION TESTS OF Ni<sub>3</sub>Al BASED INTERMETALLIC ALLOY BY USING THE SPLIT HOPKINSON PRESSURE BAR TECHNIQUE

P. Jozwik<sup>a\*</sup>, M. Kopec<sup>b</sup>, W. Polkowski<sup>c</sup>, Z. Bojar<sup>a</sup>

<sup>a\*</sup> Military University of Technology, Faculty of Advanced Technologies and Chemistry, Warsaw, Poland

<sup>b</sup> Institute of Fundamental Technological Research, Polish Academy of Sciences, Warsaw, Poland

<sup>c</sup> Foundry Research Institute, Centre for High Temperature Studies, Cracow, Poland

(Received 13 November 2018; accepted 28 January 2019)

### Abstract

In this work, the Ni<sub>3</sub>Al-based intermetallic alloy was subjected to room temperature dynamic plastic deformation tests by using a split Hopkinson pressure bar technique. The dynamic compression processes were carried out at strain rates in the range of  $\dot{\epsilon} = (1.9 \times 10^2 \div 1 \times 10^4 \text{ s}^{-1})$ . A strong impact of applied deformation conditions on microstructure and mechanical properties evolution in the examined Ni<sub>3</sub>Al intermetallic, was documented. Generally, very high maximum compressive stress values were obtained, reaching 5500 MPa for the sample deformed at the highest strain rate (i.e.  $\dot{\epsilon} = 1 \times 10^4 \text{ s}^{-1}$ ). The results of performed SEM/EBSD evaluation point towards an occurrence of dynamic recovery and recrystallization phenomena in Ni<sub>3</sub>Al samples deformed at high strain rates.

**Keywords:** Ni<sub>3</sub>Al-based alloy; Split Hopkinson pressure bar; SEM/EBSD analysis

### 1. Introduction

Ni<sub>3</sub>Al-based intermetallic alloys exhibit a set of physical and chemical properties that are highly competitive to other high-performance metallic materials e.g. a positive yield strength vs. temperature dependence, a relatively low density, an excellent corrosion resistance, and a good catalytic performance as well [1-3]. Aforementioned properties have already resulted in few successful applications of nickel aluminides, mostly in the metallurgical processing sector [1, 2]. Nevertheless, for a long time wide industrial implementation of these materials encountered many technological obstacles, mainly related to their insufficient plasticity and a tendency to brittle cracking. However, a prominent progress in design, fabrication and processing of Ni<sub>3</sub>Al intermetallics has taken place in recent years. It has been already documented that a modification of chemical composition (i.e. alloying with boron and zirconium) [4], combined with a properly tailored multi-stage thermomechanical treatment (including cold-rolling and intermediate annealing) allows substantially overcoming the problem of intermetallics brittleness. Nowadays, fine-grained

polycrystalline Ni<sub>3</sub>Al-based tapes and strips obtained by a thermo-mechanical treatment developed in our department show a room temperature strength/ductility ratio controlled in a wide range. It was documented [5, 6] that depending on obtained structural features the Ni<sub>3</sub>Al-based alloys combine either ultimate tensile strength (UTS) up to 2900 MPa with a small tensile elongation or the UTS of around 1100 MPa with the elongation up to 70%. In such conditions they are ready to be moved into new fields of industrial usage. The Ni<sub>3</sub>Al-based alloys in the form of cold rolled sheets and foils have been identified as competitive candidates in various hi-tech aerospace, automotive or military applications. One of emerging idea is to introduce the Ni<sub>3</sub>Al-based sheets into a design of components subjected to impact or shock loading (e.g. as materials for ballistic armors). Indeed, preliminary ballistic tests of Ni<sub>3</sub>Al intermetallics have been already performed giving some positive results [2]. It was documented that the Ni<sub>3</sub>Al-based alloy exhibited good performance during shooting test with 7.63 mm caliber bullet. Nevertheless, high-strain-rate properties of nickel aluminides ought to be further examined in order to validate their usefulness. A split-Hopkinson pressure

\*Corresponding author: pawel.jozwik@wat.edu.pl



bar (SHPB) setup has been accepted to be used in experiments needed for such verification [7].

Although, there is a great number of papers on static or quasi-static tensile and compression behavior of Ni<sub>3</sub>Al-based alloys [8-12], a very limited information is reported on mechanical response of nickel aluminides deformed under dynamic conditions. To our best knowledge, the only available papers on this matter are authored by Grey et al. [13, 14] which present the results of Ni<sub>3</sub>Al alloys fabricated by a powder metallurgy approach, and subjected to compression tests at strain rates up to 10<sup>3</sup> s<sup>-1</sup> and under the true strain limited to 0.2.

Therefore, the main aim of this study is to examine mechanical behavior and structural evolution of fine-grained polycrystalline boron and zirconium doped Ni<sub>3</sub>Al-based alloy upon high-strain rate compression tests performed by using a SHPB setup.

## 2. Experimental

The material investigated was Ni<sub>3</sub>Al(Zr,B) alloy with a nominal chemical composition of Ni-11.7Al-0.4Zr-0.03B (wt. %). The material was fabricated from pure elements by melting and casting in a vacuum induction furnace. The as-cast ingots were subjected to a preliminary cold-rolling to 50% of thickness reduction followed by a post-deformation annealing treatment at 1000°C, in argon atmosphere (more details on applied treatments are shown elsewhere [5]). Subsequently, cylindrical specimens having diameter of 4 mm and height of 2 mm, were electro-discharge machined from the obtained plates for the dynamic deformation tests.

The high-strain-rate compression tests at strain rate in the range of 10<sup>2</sup> to 10<sup>4</sup> s<sup>-1</sup> were carried out at room temperature by using a conventional SHPB setup that is described elsewhere in details [15]. The experimental SHPB setup was equipped with a striker, incident and transmitter bars made of the high-strength maraging steel. Diameter and length of incident and transmitter bars were 20 mm and 1000 mm, respectively. The following strain rates were applied upon the room temperature compression tests: 1.9×10<sup>2</sup>; 3.7×10<sup>3</sup>; 4.1×10<sup>3</sup>; 6.5×10<sup>3</sup>; 1×10<sup>4</sup> s<sup>-1</sup>.

The as-deformed samples were cut along their deformation axis (corresponding to the compression direction) by using the EDM device and then subjected to a structural characterization. The applied metallographic procedure included mechanical grinding on SiC papers followed by polishing with 3-1 μm diamond and 0.1 μm silica suspensions. Microstructural examinations were carried out by using FEI Quanta 3D field emission gun scanning electron microscope (FEG-SEM), equipped with electron backscatter diffraction system (EBSD). During acquisition of EBSD scans (each of them

having at least 75000 measurement points) a step size of 0.2 μm was applied. The post-processing of collected EBSD data was performed by using TSL Analysis 5 commercial software.

In order to quantify structural effects of applied straining conditions, the EBSD technique was used to determine fractions of low and high angle grain boundaries (LAGBs<15° and HAGBs>15°, respectively [16]), an average grain orientation spread (GOS<sub>av</sub>) [17,19] and image quality (IQ) values [17,19].

## 3. Results and discussion

### 3.1. High-strain-rate compression tests

The results of high strain-rate compression test point towards a high strain-rate sensitivity of examined Ni<sub>3</sub>Al-based alloy for the sample compressed at the lowest strain rate ( $\dot{\epsilon} = 1.9 \times 10^2$  s<sup>-1</sup>), where the maximum stress value of 1200 MPa was recorded. On the other hand, rising the strain rate resulted in intensive increase of maximum stress values that reached even up to 5500 MPa for the maximum applied strain rate ( $\dot{\epsilon} = 1.0 \times 10^4$  s<sup>-1</sup>) (Fig. 1). What should be noted, even for such dynamic straining conditions, the height reduction of 60% was obtained without visible evidence of cracking.

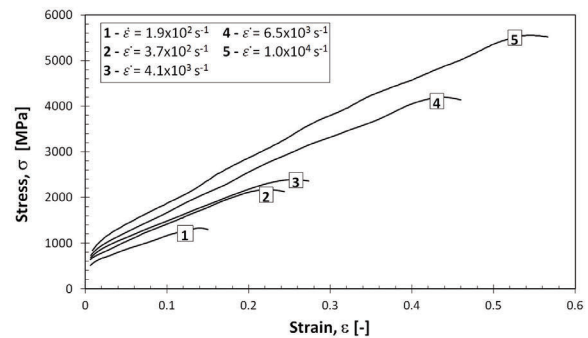


Figure 1. Stress-strain curves recorded at room temperature deformation of Ni<sub>3</sub>Al-based alloy at various strain rates

The results obtained in compression tests were subsequently used to compute values of strain rate sensitivity parameter  $m$ , according to the following formula:

$$m = \frac{\log \frac{\sigma_2}{\sigma_1}}{\log \frac{\dot{\epsilon}_2}{\dot{\epsilon}_1}} \quad (1)$$

where:  $\sigma_1$ ,  $\sigma_2$  denote stress values recorded at corresponding  $\dot{\epsilon}_1$  and  $\dot{\epsilon}_2$  strain rates. By taking into account that different strain values were obtained for various strain rates, the  $m$  parameter was calculated

only for strain  $\varepsilon \leq 0.08$ .

The increase of applied strain rate was assisted by apparently higher stress values recorded during the SHPB experiment, leading also to an increase of the calculated values of the  $m$  parameter (Fig. 2). Furthermore, the  $m$  value was almost constant within the examined strain range of  $\varepsilon \leq 0.08$ , for each particular strain rate value.

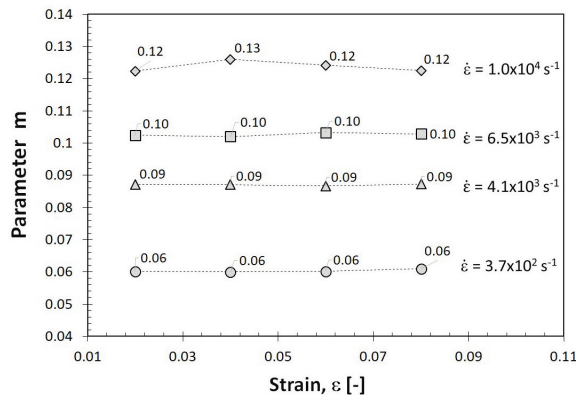


**Figure 2.** Changes of strain rate sensitivity parameter  $m$  of  $Ni_3Al$ -based alloy versus strain level

Interestingly, the values of maximum compressive stress obtained in the present work are few times higher than these reported by Sizek and Grey [13] for a binary  $Ni_3Al(B)$  alloy tested with the SHPB device. The aforementioned authors documented that for the material deformed with strain rate  $8000 \text{ s}^{-1}$  (at room temperature), the highest maximum stress value was only  $\sim 1300 \text{ MPa}$ . Such large differences between the results presented here and in the literature, should be justified by:

- (i) a substantially higher total accumulated strain obtained in the present work ( $\varepsilon_t = 0.54$  vs.  $\varepsilon_t = 0.12$ );
- (ii) different applied fabrication methods: casting + thermomechanical treatment (this work) vs. powder metallurgy approach ([13]);
- (iii) the addition of zirconium to presently examined alloy – this element significantly increases effectiveness of the solid solution strengthening via substitution of aluminum atoms in the  $Ni_3Al$  crystal lattice [17].

Furthermore, a strong impact of the strain rate on yield stress value was recorded in the present work. It is found that the yield strength increased from  $\sim 500 \text{ MPa}$  to  $\sim 850 \text{ MPa}$  when the applied strain rate was  $\dot{\varepsilon} = 1.9 \times 10^2 \text{ s}^{-1}$  and  $\dot{\varepsilon} = 1.0 \times 10^4 \text{ s}^{-1}$  respectively. It should be noted, that such behavior is not usual in the case of f.c.c. metals having a high stacking fault energy, and is quite different to that reported by Sizek et al. [13].

Generally, room temperature plastic deformation process of  $Ni_3Al$  alloys carried out under static (or semi-static) conditions proceeds similarly to that in high stacking fault energy f.c.c. metals. It means that the main involved deformation mechanism is dominated by octahedral slip on closed-packed  $\{111\}$  planes and along closed-packed  $\langle 110 \rangle$  direction. This glide system is characterized by a lack or low strain-rate sensitivity of yield stress as a partial consequence of low density of Peierls barriers. An increase of temperature initiates the cross slip of screw dislocations to  $\{100\}$  planes, which provides much higher density of Peierls barriers, resulting in a high strain rate sensitivity. Sizek et al. reported [13] that the room temperature yield stress in the  $Ni_3Al$  alloy exhibits a little or no strain rate sensitivity, but increasing strain temperature above  $550^\circ\text{C}$  provides more visible changes of the yield stress. It should be added that the authors [13] applied the maximum strain of  $\varepsilon \leq 0.12$  (at room temperature) which was 4.5 lower than that in the present work [13]. A higher level of plastic strain enables an activation of mechanical twinning [14] as well as generates much more heat leading to increase of sample's temperature (even above  $550^\circ\text{C}$ ). Such high sample temperature allows the activation of dislocation slip in the  $\{100\}\langle 110 \rangle$  cubic system which is more typical for b.c.c. crystals.

### 3.2 Microstructure evolution

The  $Ni_3Al(Zr,B)$  alloy in the initial state was characterized by a single phase ( $\gamma'$ ) composition, and equiaxed microstructure with an average grain size of  $\sim 10 \mu\text{m}$  (Fig. 3a-c). The results of EBSD examinations revealed typical features of as-annealed metals, i.e. almost complete lack of LAGBs inside grains interior and corresponding very low GOS values (the average  $GOS_{av}$  value was below 1).

The room temperature dynamic compression of the  $Ni_3Al(Zr,B)$  intermetallic resulted in an intensive structural evolution which was increasing with increasing the applied strain rate. The sample cold deformed at the lowest strain rate ( $\dot{\varepsilon} = 1.9 \times 10^2 \text{ s}^{-1}$ ) showed only slight increase of LAGBs fraction (Fig. 3d) and the average GOS value (from  $GOS_{av} = 0.5$  to  $GOS_{av} = 3.7$ ) (Fig. 4a), as compared to the material in its initial state. Much more extensive structural changes were observed for samples compressed at higher strain rates. Starting from  $\dot{\varepsilon} = 3.7 \times 10^3 \text{ s}^{-1}$  (Fig. 3. g-i), a significant change of grains morphology (from equiaxed to elongated ones) and an increase of LAGBs fraction and grain orientation spread ( $GOS_{av} = 8.1$ ) were noted. This tendency was generally maintained upon a further increase of the strain rate up to  $\dot{\varepsilon} = 6.5 \times 10^3 \text{ s}^{-1}$ . However, it should be noted that the sample subjected to compression at the



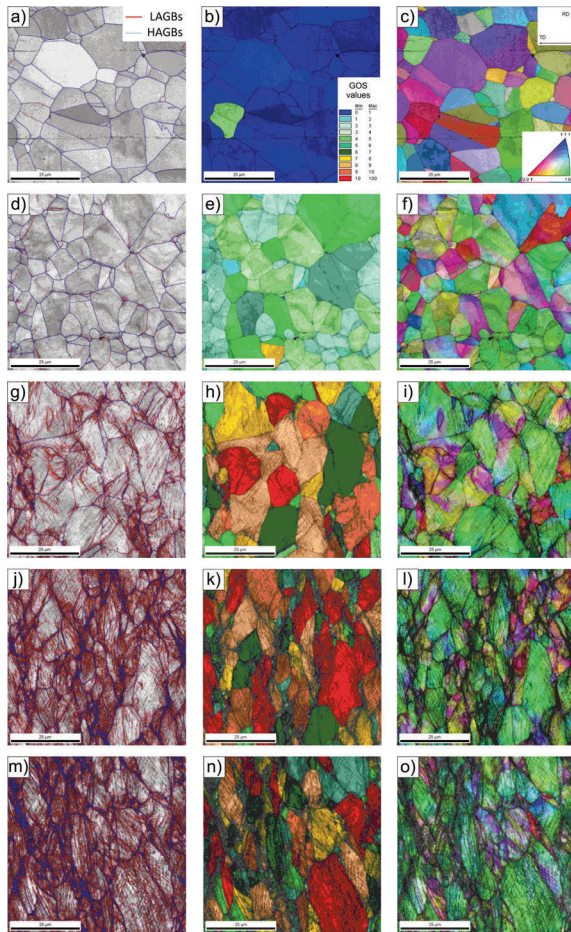


**Figure 3.** Examples of EBSD images obtained for investigated  $\text{Ni}_3\text{Al}$ -based alloy: initial stage – a–c) and after dynamic compression at room temperature with deformation speed  $\dot{\epsilon}$ : d–f)  $1.9 \times 10^2 \text{ s}^{-1}$ ; g–i)  $3.7 \times 10^3 \text{ s}^{-1}$ ; j–l)  $6.5 \times 10^3 \text{ s}^{-1}$ ; m–o)  $1.0 \times 10^4 \text{ s}^{-1}$  (a,d,g,j,m – IQ maps with LAGBs and HAGBs visualization; b,e,h,k,n – GOS maps; c,f,i,l,o – IPF maps)

highest considered strain rate ( $\dot{\epsilon} = 1.0 \times 10^4 \text{ s}^{-1}$ ) breaks the inclination on diagram presented in Fig. 4a. The slightly lowered  $\text{GOS}_{\text{av}}$  value measured for this sample points towards a possible occurrence of dynamic recovery and even early stages of recrystallization.

Above described evolution of the GOS parameter is in line with changes of the relative IQ values (Fig. 4b). It is documented that increase of the strain rate up to  $\dot{\epsilon} = 3.7 \times 10^3 \text{ s}^{-1}$  results in almost linear decrease of the relative IQ. For higher strain rates, the relative IQ values seem to be stabilized at constant level.

Summing up the evolution of the GOS parameter, it is worth noting that its concept is based on the assumption that plastic deformation in a polycrystalline metallic material causes local changes in the orientation of the crystal lattice in the volume of individual grains. Such local crystal lattice rotations are necessary to preserve the integrity of the material subjected to plastic deformation. Therefore, along with the increase in the degree of plastic deformation, the value of the GOS parameter also increases (compare Fig. 3 b, e, h, k, and n). In the material after dynamic plastic deformation (starting from  $\dot{\epsilon} = 3.7 \times 10^3 \text{ s}^{-1}$ ) grains with a GOS value from the range of 8–10 dominate, in contrast to the starting material (after recrystallization), where grains with  $\text{GOS} < 1$  are definitely dominant.

#### 4. Conclusions

Based on the results of high-strain-rate compression tests of the  $\text{Ni}_3\text{Al}$  alloy carried out at room temperature by using a conventional SHPB setup, the following conclusions are drawn:

1. The examined  $\text{Ni}_3\text{Al}$  alloy exhibits a high strain rate sensitivity – along with the increase of the strain rate, the value of m also increases.
2. The increase of strain rate results in the

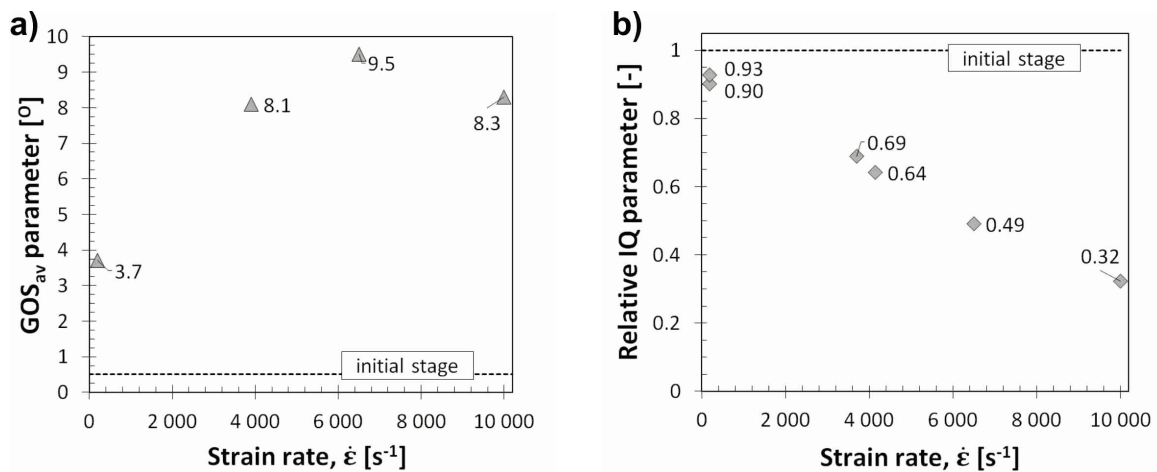


**Figure 4.** The results of quantitative EBSD analyses obtained for the investigated material: a) average GOS parameter, b) relative IQ parameter values

intensive strain hardening reflected by a substantial rise of the maximum stress values (up to 5500 MPa for the  $\dot{\varepsilon} = 1.0 \times 10^4 \text{ s}^{-1}$ ) without formation of any visible cracks. However, the increase of strain rates was also accompanied by achievement of higher true strain values, thus the observed changes should be considered in terms of a superposition of strain rate and true strain effects.

3. The increase of the strain rate has a strong impact on the evolution of microstructure in the examined Ni<sub>3</sub>Al alloy reflected by the change of grain shape, the formation of slip bands, and the increase of both, LAGBs fraction and average GOS values.

4. The sample subjected to compression at  $\dot{\varepsilon} = 6.5 \times 10^3 \text{ s}^{-1}$  was characterized by a slightly lowered fraction of grains having high GOS values (and thus the lower average GOS). This finding might be related to a possible occurrence of local structure restoration phenomena such as dynamic recovery and recrystallization.

### Acknowledgements

*The authors acknowledge MSc. Eng. Michal Piszcz for the help with preparation of EBSD results. Financial support from the Polish National Centre for Research and Development under grant No. 246 201 is gratefully acknowledged.*

### References

- [1] S.C. Deevi, V.K. Sikka, *Intermetallics* 4 (1997) 357-375.
- [2] P. Jozwik, W. Polkowski, Z. Bojar, *Materials* 8 (2015) 2537-2568.
- [3] R. Mitra, R.J.H. Wanhill: *Structural Intermetallics*, in: N. Prasad, R. Wanhill, *Aerospace Materials and Material Technologies*, vol. 1: *Aerospace Materials*, Indian Institute of Metals Series. Springer, Singapore, 2017, pp. 229-245.
- [4] K. Aoki, O. Izumi, *Nippon Kinzoku Gakkaishi* 43 (1979) 1190-1196.
- [5] P. Jozwik, Z. Bojar, *Arch. Metall. Mater.* 52, 2 (2007) 321-327.
- [6] P. Jozwik, Z. Bojar, *Eng. Sci.* 27 (2006) 753-756.
- [7] Y. Gu, V.F. Nesterenko, S. S. Indrakanti, *Proc. AIP Conf.* 620, 2002, p.1294.
- [8] Y. Wu, Y. Liu, Ch. Li, X. Xia, Y. Huang, H. Li, H. Wang, *J. Alloys Comp.* 712 (2017) 687-695.
- [9] J. Malcharcziková, M. Kursá, M. Pohludka, P. Kawulok, P. Gratzá, *Proc. 26th Int. Conf. on Metall. Mater., METAL 2017*, pp. 1874-1880.
- [10] S. Kobayashi, M. Demura, K. Kishida, T. Hirano, *Intermetallics* 13, 6 (2005) 608-614.
- [11] I. Schindler, J. Macháček, M. Spittel, *Intermetallics* 7, 1 (1999) 83-87.
- [12] I. Schindler, J. Machacek, J. Kliber, M. Greger, M. Kursá, *J. Mater. Proc. Technol.* 60 (1996) 575-580.
- [13] H.W. Sizek, G.T. Gray III, *Acta Metall. Mater.* 41 (1993) 1855-1860.
- [14] D. E. Albert, G.T. Gray III, *Phil. Mag. A* 70 (1994) 145-158.
- [15] W. Močko, Z.L. Kowalewski, *Journal of Kones* 19 (2012) 345-351.
- [16] P. Lejček, *Grain Boundaries: Description, Structure and Thermodynamics*, in: R. Hull, C. Jagadish, R.M. Osgood, Jr., J. Parisi, Z. Wang, H. Warlimont, *Materials Science* vol. 136, Springer Heidelberg Dordrecht, London, 2010, pp.5-24.
- [17] E.M. Lehockey, Y. Lin, O.E. Lepik, *Mapping residual plastic strain in materials using electron backscatter diffraction*, in A.J. Schwartz (Ed.) et al.: *Electron Backscatter Diffraction in Materials Science*, Kluwer Academic/Plenum Publishers (2000) 247-264.
- [18] W. Polkowski, P. Jóźwik, K. Karczewski, Z. Bojar, *Arch. Civ. Mech. Eng.* 14 (2014) 550-560.
- [19] A.J. Wilkinson, *Acta Metall. Mater.* 39 (1991) 3047-3055.



## ISPITIVANJE DINAMIČKIH DEFORMACIJA KOD $\text{Ni}_3\text{Al}$ INTERMETALNE LEGURE TEHNIKOM RAZDVOJENE HOPKINSONOVE POLUGE POD PRITISKOM

P. Jozwik<sup>a\*</sup>, M. Kopec<sup>b</sup>, W. Polkowski<sup>c</sup>, Z. Bojar<sup>a</sup>

<sup>a\*</sup> Vojni tehnološki univerzitet, Fakultet za napredne tehnologije i Hemiju, Vršava, Poljska

<sup>b</sup> Institut za tehnološko istraživanje, Poljska akademija nauka, Varšava, Poljska

<sup>c</sup> Institut za izučavanje postupaka livenja, Centar za izučavanje visokih temperatura, Krakov, Poljska

### Apstrakt

U ovom radu je ispitivana dinamička plastična deformacija na sobnoj temperaturi kod  $\text{Ni}_3\text{Al}$  intermetalne legure tehnikom razdvojene Hopkinsonove poluge pod pritiskom (SHPB). Postupci dinamičkog sabijanja su izvedeni sa deformacijama pri istezanju u opsegu  $\dot{\epsilon} = (1.9 \times 10^2 \div 1 \times 10^4 \text{ s}^{-1})$ . Zabeležen je veliki uticaj primenjenih uslova za deformaciju na mikrostrukturu, kao i na razvoj mehaničkih osobina kod ispitivanih  $\text{Ni}_3\text{Al}$  intermetalnih legura. Uglavnom su dobijene veoma visoke vrednosti za pritisak naprezanja, gde je za uzorak deformisan pri najvišoj vrednosti istezanja iznosio 5500 MPa (t.j.  $\dot{\epsilon} = 1 \times 10^4 \text{ s}^{-1}$ ). Rezultati koji su ispitani SEM/EBSD postupkom ukazuju na postojanje fenomena dinamičkog obnavljanja i rekristalizacije u uzorcima  $\text{Ni}_3\text{Al}$  koji su deformisani pri visokim vrednostima istezanja.

**Ključne reči:**  $\text{Ni}_3\text{Al}$  legure; Razdvojena Hopkinsonova poluga pod pritiskom; SEM/EBSD analiza

